Stress gradient effect in HCF for notched components taking into account cyclic plasticity

Thierry PALIN-LUC[a], Nicolas SAINTIER[a] and Jean-François FLAVENOT[b]

[a] ENSAM, Université Bordeaux 1, LAMEFIP (EA2727), Esplanade des Arts et Métiers, F-33405 Talence Cedex, France
[b] CETIM, 52 Av. Félix Louat, BP 80067 – 60304 Senlis Cedex, France

Abstract Most fatigue crack initiations on components are related to notches. The fatigue strength assessment of notched components is difficult because of stress-strain gradients and macroscopic plastic strains at the notch root. In this paper, a non-local energy based multiaxial fatigue criterion is used to assess the fatigue strength of notched specimens made of 42CrMo4 quenched and tempered steel under tension and rotating bending. The stabilized stress-strain state is computed by cyclic elastic-plastic FEA. A cyclic mechanical behaviour combining both a constant isotropic hardening and a non-linear kinematic hardening is identified from low-cycle fatigue tests. The predictions of the non-local approach with elastic-plastic calculations are significantly better than the elastic ones and allow the authors to discuss the need of both a volumetric approach and elastic-plastic FEA.

1 INTRODUCTION

Fatigue crack initiation on components is usually arising around notches where gradients and high stress-strain levels are encountered. Two major difficulties can be identified when dealing with fatigue strength assessment in such cases: to compute the cyclic stress strain state at the notch where macroscopic plastic strains take place and to take into account the stress/strain distribution (gradients, "supporting effect"). The following sections aim to present the approach proposed in this study. First, we will present the computation of the stress strain distribution and history under various loading types in order to state on the elastic shake-down or plastic shake-down processes taking place at the notch root. Secondly, the fatigue strength assessment of notched specimens using a non-local energy based criterion is proposed.

2 EXPERIMENTS

2.1 Material

The material is a 42CrMo4 quenched and tempered steel which mechanical properties under quasi-static tension are given Table 1.

Table 1. Basic 42CrMo4 mechanical properties.

Rp0.2 (MPa)	928
Rm (MPa)	1024
E (MPa)	207
ν	0.3

2.2 Specimen geometry and fatigue test results

All mechanical testing were performed at CETIM. Fatigue tests were carried out under load control on a resonant testing machine (vibrophore). The stopping criterion was a decrease of the resonance frequency which corresponds to a crack of a few millimeters. The experimental fatigue limits at 10^7 cycles (for a probability of 0.5, staircase method) are given in Table 2 in nominal stress (σ_m is the mean stress, σ_a is the amplitude). The specimen geometries used for rotating bending tests (resp. tension tests) are illustrated in Figure 1 (resp. Figure 2).

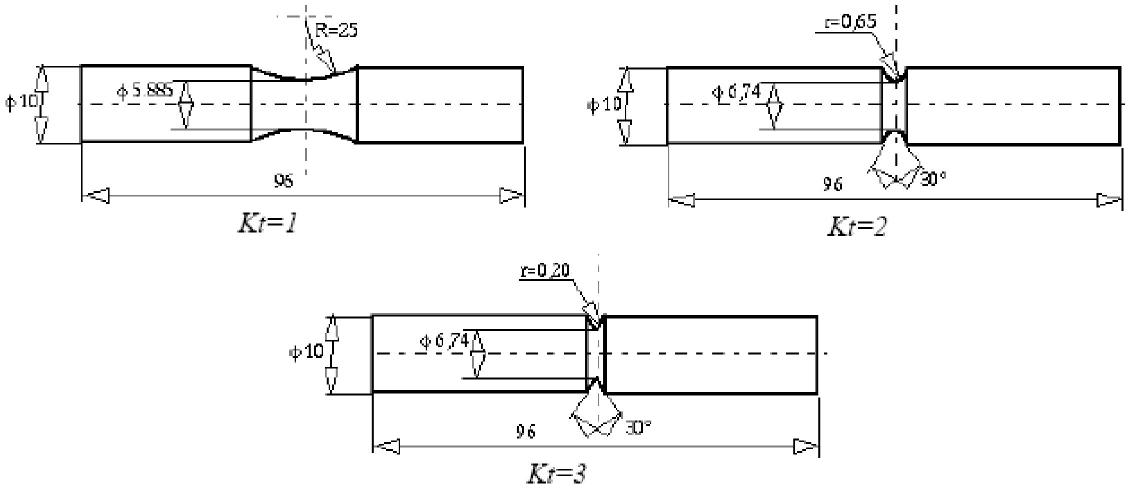

Figure 1: Specimen geometries for rotating bending fatigue tests.

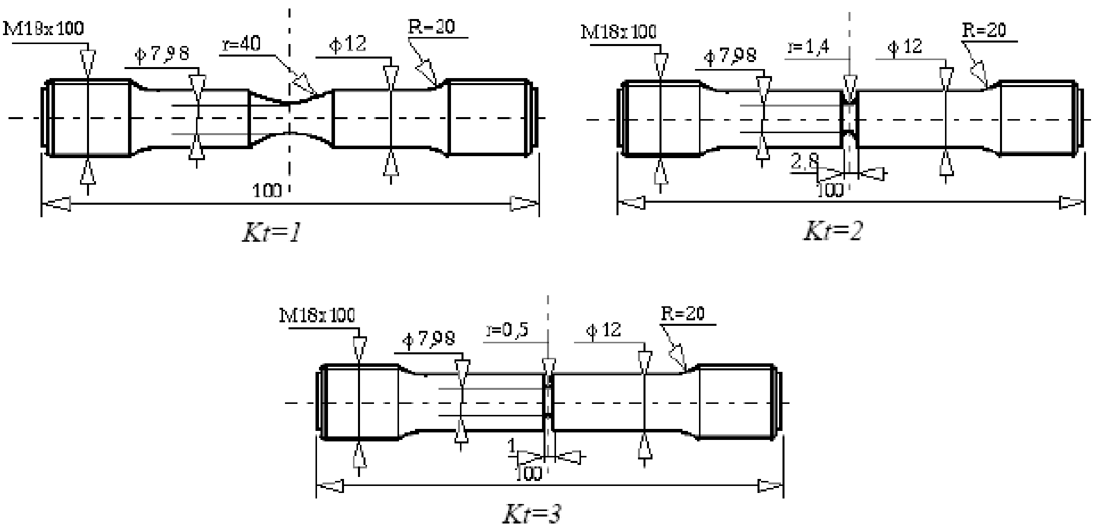

Figure 2: Specimen geometries for tension fatigue tests

3 AN ENERGY BASED NON-LOCAL MULTIAXIAL FATIGUE CRITERION

Any criteria expressed only as a function of local variables (such as stress or strain tensors) at a point can not distinguish load types and predict stress-strain gradient effect because they do not take into account the distribution of stresses: non-local effect can not be taken into account. According to the authors a good fatigue criterion has to consider the stress-strain distribution in a volume related to the microstucture and/or the loading type. Palin-Luc et al. [6], Banvillet et al. [1] and Bénabes et al. [2] proposed the concept of volume influencing fatigue crack initiation around the critical point (with regard to fatigue) in order to take into account such non-local effects. The driving force for damage initiation and growth, up to fatigue crack initiation at the macroscale (typical fatigue crack size 1 mm) considered here is the strain work density given to each elementary volume of material per loading cycle, *Wg* given by Eq (1).

$$Wg(M) = \sum_{i,j} \int_T \left\langle \sigma_{ij}(M,t)\dot{\varepsilon}_{ij}(M,t) \right\rangle dt \quad (1)$$

where <a> = a if a > 0 and <a> = 0 if a ≤ 0 and (.) denotes the time derivative.

Table 2. Median fatigue limits at 10^7 cycles of 42CrMo4 specimens.

Loading	Kt	$\sigma^D_{m,nom}$ (MPa)	$\sigma^D_{a,nom}$ (MPa)
Tension	1	0	508
Tension	1	400	468
Tension	2	500	252
Tension	3	0	220
Tension	3	500	165
Rotating Bending	1	0	540
Rotating Bending	2	0	267
Rotating Bending	3	0	180
Torsion	1	0	320

This parameter is equal to the integral over a loading cycle of the positive part of the strain power density; this is also equal to the positive variation of the potential strain energy density over a loading period [1]. *Wg* is computed from elastic strains after the elastic shakedown of the material which is supposed to occur in high cycle fatigue. Indeed, usually the fatigue limit is low enough to consider that the material remains elastic at the macroscopic scale [4]. As it will be shown in the following section, numerical computations show that in some loading cases the elastic shake-down behaviour is not reached but a plastic shake-down (accommodation) is rather obtained. In that case, in a first approach, we will only consider the elastic part of the accommodated cycle to compute the fatigue damage parameter. The plastic part will be neglected. It has to be noticed that *Wg* is not shape dependent (sinus, triangle, square, etc.), this is in agreement with Ref. [9].

3.1 Volume influencing fatigue crack initiation and threshold stress concepts

To predict the effect on the fatigue limit of the stress-strain distribution inside the component, a volume influencing fatigue crack initiation, V*, is considered [1, 2, 3, 6]. Under fully reversed uniaxial stress state, this volume is defined by the set of points where the stress amplitude is higher than a material dependent threshold stress σ^*. From fully reversed fatigue experiments, Palin-Luc et al. [5] showed that a threshold stress, σ^*, can be defined below the usual fatigue limit σ^D (asymptotic value of the S-N curve). At a material point, a stress amplitude lower than this threshold does not initiate observable damage at the mesoscopic scale (no micro-crack). A stress amplitude between σ^* and σ^D contributes to meso-damage initiation only (micro-crack in one or some grains), which could develop if, either near this point or in the course of time there is a stress amplitude higher than σ^*. The stress σ^* is considered as a threshold stress of no damage initiation at the mesoscopic scale, whereas the fatigue limit σ^D is seen as a macro-crack initiation (or technical crack) threshold. By reference to an homogenous fully reversed uniaxial stress state (tension on smooth specimen) the threshold value of *Wg* corresponding to σ^* is: $Wg^* = (\sigma^*)^2/E$, where *E* is the Young modulus of the material. The volume influencing fatigue crack initiation is then defined by (2) around each critical point Ci (where *Wg* reaches a local maximum). Over this volume, the damaging parameter is the mean value of the strain work density given to the material exceeding the threshold *Wg** (3). This damaging strain work density is supposed to be constant for a material loaded at its fatigue limit under uniaxial stress state.

$$V^*(Ci) = \{\text{points } M(x,y,z) \text{ around } Ci \text{ so that } Wg(M) \geq Wg^*\} \quad (2)$$

$$\varpi_g(C_i) = \frac{1}{V^*(C_i)} \iiint_{V^*} \left\langle W_g(M) - W_g^{\ *} \right\rangle dv \quad (3)$$

3.2 Multiaxial fatigue criterion

Under uniaxial stress state, the condition for no fatigue crack initiation is thus $\varpi_g(C_i) \le \varpi^D_{g,uniax}$, where $\varpi^D_{g,uniax}$ is the value of ϖ_g at the fatigue limit for an uniaxial stress state. By applying this hypothesis with the fatigue limits under fully reversed tension $\sigma^D_{-1,tens}$ and rotating bending $\sigma^D_{-1,rotbend}$ on smooth specimens, the threshold stress σ* can be identified (4) [1, 6]. The value of $\varpi^D_{g,uniax}$ is identified according to eq.(5) by assuming that its value is constant for any loading under uniaxial stress state.

$$\sigma^* = \sqrt{2\left(\sigma^D_{-1,tens}\right)^2 - \left(\sigma^D_{-1,rot.bend}\right)^2} \tag{4}$$

$$\varpi^D_{g,uniax} = \frac{\left(\sigma^D_{-1,rot.bend}\right)^2 - \left(\sigma^D_{-1,tens}\right)^2}{E} \tag{5}$$

For a multiaxial stress state at the fatigue critical point, a multiaxial correction is used as proposed in [1, 6, 7]. The triaxiality degree of stresses dT(M) is defined by the ratio between the strain work density Wg^{Sph} due to the spherical part of the stress tensor (corresponding to the hydrostatic stress) and Wg (6). This ratio varies between 0 (pure distorsion) and 1 (pure equitriaxial stress state).

$$dT(M) = \frac{W_g^{Sph}(M)}{W_g(M)} \tag{6}$$

The influence of the stress triaxiality is considered by computing the strain work density given to the material within the volume V* which is equivalent to a uniaxial stress state, $Wg_{eq}(M)$. In eq. (8) $dTuniax$ is the value of dT for a uniaxial stress state; F is an empirical function depending on both dT(M) and a material dependent parameter β (see [7, 8] for details). This last parameter is representative of the material sensitivity to the stress triaxiality; its identification has to be done by applying equation (9) with the two fully reversed endurance limits on smooth specimens: in rotating bending and in torsion.

$$Wg_{eq}(M) = Wg(M)\frac{F(dTuniax,\beta)}{F\left(dT(M),\beta\right)} \tag{8}$$

$$F\left(dT(M),\beta\right) = \frac{1}{1-dT(M)}\left\{1-\frac{1}{\beta}\ln\left[1+dT(M)\left(\exp(\beta)-1\right)\right]\right\} \tag{9}$$

Then, under multiaxial stress state, or whatever the stress state is, the damage parameter $\varpi_{geq}(C_i)$ is computed from eq. (10). It has to be understood as the mean value in the volume influencing fatigue crack initiation of the damaging strain work density which is equivalent to a uniaxial stress state at the critical point.

$$\varpi_{g,eq}(C_i) = \frac{1}{V^*(C_i)}\iiint_{V^*}\left\langle W_{g,eq}(M) - W_g^{\ *}\right\rangle dv \tag{10}$$

This quantity depends on the stress state at C_i and on the distribution of stress-strain inside $V^*(C_i)$. That is the reason why the stress-strain gradient effect is considered. To prevent fatigue crack initiation at the critical point for any stress states, loadings and stress-strain gradients, the non-local multiaxial fatigue criterion is: $\varpi_{g_{eq}}\left(C_i\right) \leq \varpi_{g,uniax}^{D}$. Let us recall, the damage parameter at the fatigue limit $\varpi_{g,uniax}^{D}$ is identified from two fully reversed fatigue limits on smooth specimens according to eq. (5).

4 NUMERICAL SIMULATION

4.1 Finite element analysis conditions

All simulations were performed at the LAMEFIP using the ZéBuLoN finite element code (CdM, Ecole des Mines de Paris).

Mesh

For this study, 20 nodes 3D quadratic elements were used for all numerical computation. A mesh example is given figure 3.

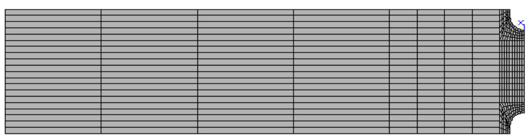

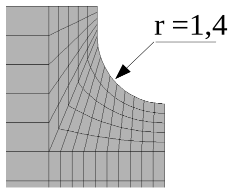

a) Cut in plane $\left(O, \vec{x}_1, \vec{x}_2\right)$ b) Zoom on the notch in plane $\left(O, \vec{x}_1, \vec{x}_2\right)$

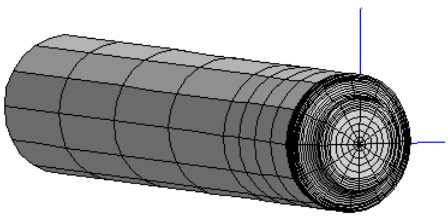

c) Global vue

Figure 3 : Mesh example for tension specimen, Kt=2.

Elastic-plastic mechanical behaviour

The material constitutive behaviour was considered as elastic-plastic using linear isotropic elasticity and non linear kinematic hardening model (Armstrong Frederick model) assuming the material follows the Von Mises plastic flaw criterion. Material parameters were identified from a set of stabilized (half life) stress-strain hysteresis loops (low-cycle fatigue tests) obtained on smooth specimens under strain control fully reversed tension (R_ε=-1, $\dot{\varepsilon}= 4.\,10^{-2} s^{-1}$). The following constitutive equations were used:

$$f\left(\sigma, X\right) = \sigma_{eq}\left(\sigma - X\right) - R \tag{11}$$

$$\dot{\alpha} = \dot{\lambda}\left(n - \frac{3}{2}\frac{D}{C}X\right) \text{and } X = \frac{2}{3}C\alpha \tag{12}$$

The optimized behaviour is illustrated Figure 4 (E=180 GPa, ν=0.3, C=41740, D=117.04, R0=502.5 MPa). The optimized parameters allow to obtain satisfactory results in the investigated plastic strain amplitude range.

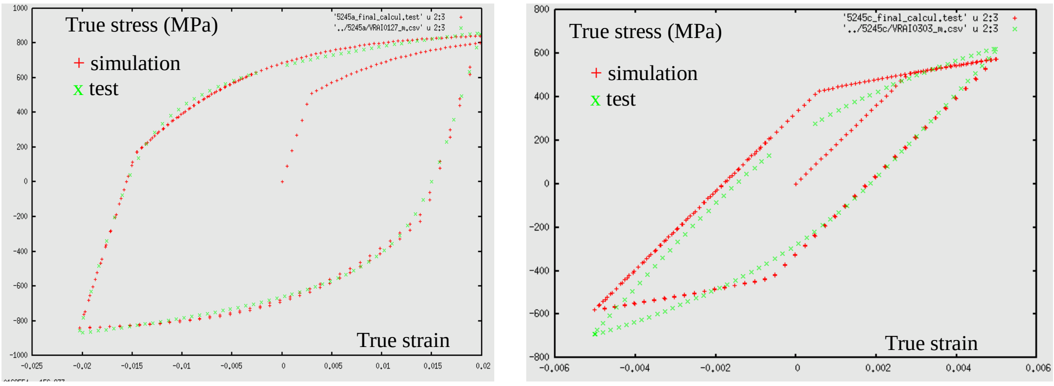

Figure 4 : Experimental and identified (numerical) cyclic behaviour (uniaxial fully reversed tension).

4.2 FEA results

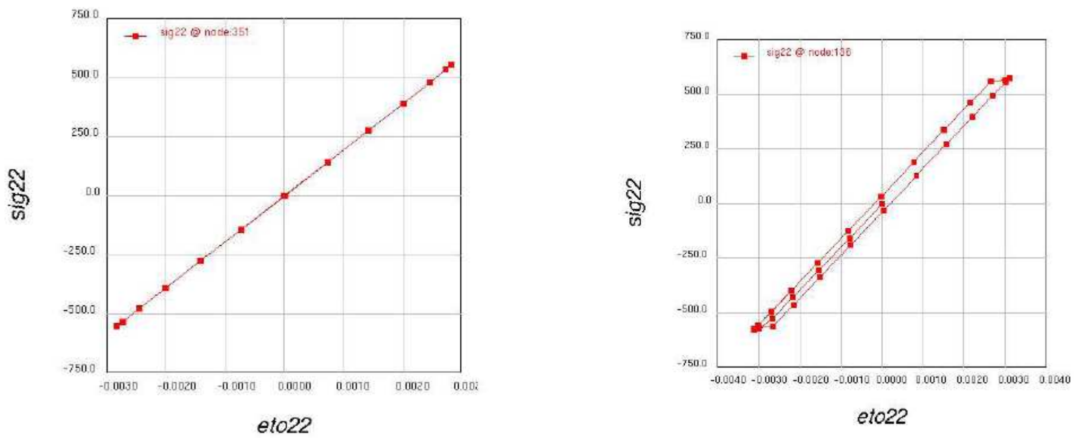

a) Kt=2 (Snom,max=267 MPa, Snom,min=-267) b) Kt=3 (Snom,max=180 MPa, Snom,min=-180)

Figure 5: Stress-strain curves (simulation) at the notch root under rotating bending loading (stress in MPa).

Figure 5 shows the local stress strain curves at the notch root for a rotating bending test under the same loading condition (rotating bending at the fatigue limit), but for two different geometries (Kt=2 and Kt=3). While the lowest Kt geometry leads to an elastic shake-down behaviour at the notch, the Kt=3 geometry shows a plastic shake-down (accommodated) behaviour. Since in this paper the proposed formulation does not consider the plastic strain work density in the damaging parameter (HCF regime), in the case of plastic shake-down only the elastic part of the stress strain history will be taken into account for fatigue strength assessment. Nevertheless, even when elastic shake-down occurs, it has to be pointed out that, due to cyclic plasticity at the notch root, the stabilized local stresses and strains computed in elastoplasticity are very different than the elastic stresses and strains. Table 2 identifies the different stabilized states or the different loading types.

5 RESULTS AND DISCUSSION

5.1 Fatigue strength assessment

Predicted fatigue limits are computed using the above proposed volumetric method (see section 2). In order to compare numerical and experimental results two parameters are given in Table 2: the usual Security Coefficient (Cs) and the Relative Error of Prediction defined by eq. (13). The calculation method is on the safety side when REP > 1 (i.e. Cs > 1). A square root is used in Cs definition to have a ratio homogeneous to stress over stress. The damage parameter $\varpi_{g,eq}$ is an energy quantity homogeneous to MPa².

$$REP = \frac{\sigma_{nom}^{D,\exp} - \sigma_{nom}^{D,pred.}}{\sigma_{nom}^{D,\exp}} \qquad \text{and} \qquad Cs = \sqrt{\frac{\varpi_{g,eq}}{\varpi_{g,eq}^{D}}} \tag{13}$$

Table 2 : Comparison of REP and Security coefficients C for purely elastic [14] and elastic-plastic computation

		Test	*Test*	*Simulation elasticity*		*Simulation elastic-plastic*		
Loading	*Kt*	*Smoy (MPa)*	*Samp (MPa)*	*Cs*	*REP (%)*	*Cs*	*REP (%)*	*Stabilized state*
Tension	1	0	508	Ref.	Ref.	Ref.	Ref.	---
Tension	1	400	467.5	1.64	26	1.44	16.5	elastic shake-down
Tension	2	500	252	2.15	68	1.08	9.5	elastic shake-down
Tension	3	0	220	1.45	16	1.23	9.5	plastic shake-down
Tension	3	500	165	2.34	80	1.32	21	elastic shake-down
Rotating bending	1	0	540	Ref.	Ref.	Ref.	Ref.	---
Rotating bending	2	0	267	0.87	-4.5	0.71	-4.5	elasticity
Rotating bending	3	0	180	1.16	5.6	1.01	~ 0	plastic shake-down
Torsion	1	0	320	Ref.	Ref.	Ref.	Ref.	---

The results obtained for an elastic-plastic behaviour are clearly better than for a simple purely elastic approach independently of the stabilized state. This confirms that a purely elastic approach can not capture the stress-strain distribution at the notch even if a non-local fatigue life criterion is used (the averaging process over a volume is not sufficient to overcome the elastic over stress at the notch). Most of the computed fatigue limits are in good agreement with the experimental results having REP values ranging from 0 to 21%. The highest REP values (21%) is obtained for the Kt=3 specimen which is found to be the specimen having the highest computed plastic strain amplitude at the notch. Some limitation of the constitutive model used in this study could partially explain this result. Futhermore, simulations lead to fatigue strength assessments lower than the experimental values (safety side) as shown by the positive REP values in Table 2.

5.2 Discussion

Table 3: Dimensions of V* for the different geometries and load cases

Loading	Kt	Fatigue limit (tests)		Elastic simulations			Elastic-plastic simulations		
		$\sigma_{m,nom}^{D}$ (MPa)	$\sigma_{a,nom}^{D}$ (MPa)	P (mm)	L/2 (mm)	V*/2 (mm^3)	P (mm)	L/2 (mm)	V*/2 (mm^3)
Tension°	1	400	467.5	3.99	5	213	3.99	6.4	322
Tension	2	500	252	0.12	0.55	1.2	0.78	0.9	11.4
Tension	3	0	220	0.04	0.22	0.16	0.07	0.3	0.335
Tension	3	500	165	0.04	0.22	0.17	0.39	0.4	3.050
Rotating bending	2	0	267	0.05	0.3	0.22	0.03	0.3	0.07
Rotating bending	3	0	180	0.015	0.1	0.022	0.02	0.13	0.02

° in such a case, all the cross section at the notch root is included in V*. P is the depth of V* along the specimen radius (see Figure 6), L is the length of V* at the notch surface (curvilinear abscissa).

Table 3 gives the dimensions of the volume V* for each load case. It is clear that due to plastic strains the volume influencing fatigue crack initiation is larger for elastic-plastic simulations than for elastic ones. The better results obtained by simulations with a cyclic elastic-plastic material behaviour show that assessment of V* volume using a purely elastic approach is not realistic. Furthermore, as seen in table 3, the size of V* notably varies with the geometry and load type of specimens. This observation which results of the proposed criterion (using a threshold energy Wg*) to define the critical volume V* could be discussed in relation with the real mechanism of fatigue crack initiation. As proposed by other authors [10] in the past, the representative volume of fatigue damage process might be constant for a defined microstructure. Other experiments should be done to clarify this important point of non-local approach in fatigue.

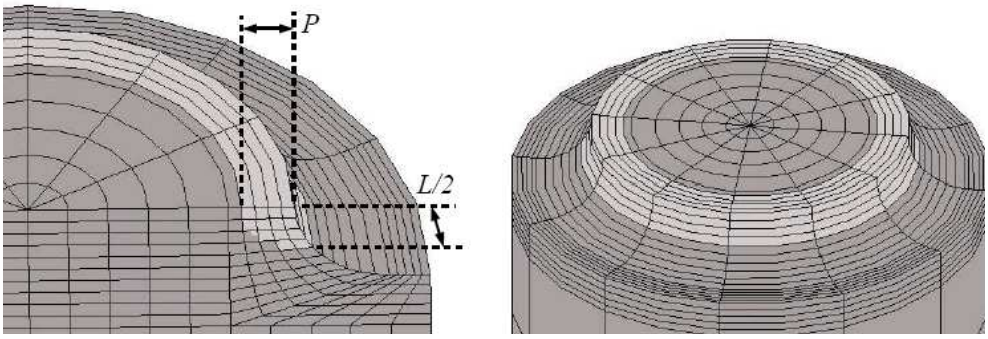

Figure 6: illustration of V* for the notched specimen Kt=2 under tension at the fatigue limit $\sigma^{D}_{m,nom}$ =500 MPa and $\sigma^{D}_{a,nom}$ =252 MPa (elastic-plastic simulation).

6 CONCLUSION AND PROSPECTS

It has been shown that elastic-plastic finite element computation are needed for fatigue strength assessment of notched components. Even with a volumetric approach to consider the gradient effect (“supporting effect”), elastic-plastic cyclic calculations have to be performed to evaluate the shake-down state. However, the cyclic plastic constitutive model identified from uniaxial test on smooth specimens may not be representative of the real material behaviour at the notch root (hydrostatic stress, gradient,…). Further experimental work is in progress in order to identify the local stress-strain behaviour for highly notched specimens and to better identify cyclic-plastic behaviour laws of the materials.

7 REFERENCES

1. A. Banvillet, T. Palin-Luc and S. Lasserre, *Int. J. Fatigue*, 25 (8), 2003, 755-769.
2. J. Bénabes, N. Saintier, T. Palin-Luc, J.-L.Charles, F. Cocheteux: An energy based multiaxial fatigue life calculation method taking into account the stress-strain gradient effect, Fatigue 2006 Conf., Atlanta, on CD Rom, Elsevier, 2006, ref FT572, 10 p.
3. T. Palin-Luc and N. Saintier, *MP Materialprüfung Materials Testing*, 49 (7-8), 2007, 370-377.
4. J. Lemaitre and J-L. Chaboche, Mécanique des matériaux solides, Bordas, Paris, 1988.
5. T. Palin-Luc and S. Lasserre and J-Y. Bérard, *Fat. Fract. Engng. Mat. Struct.*, 21, 1998, 191-200.
6. T. Palin-Luc and S. Lasserre, *Eur. J. Mech. A/ Solids*, 17 (2), 1998, 237-251.
7. A. Banvillet, Prévision de durée de vie en fatigue multiaxiale sous chargements reels : vers des essais accélérés, PhD thesis, ENSAM, France, 2003.
8. J. Bénabès, Approche énergétique non locale du calcul de durée de vie de structures en fatigue multiaxiale sous chargements d’amplitude variable. Application à une roue de train ferroviaire, PhD thesis, ENSAM, France, 2006.
9. H. Dietmann, T. Bonghibhat, A. Schmidt, Multiaxial fatigue behavior of steels under in-phase and out-of-phase loading including different wave forms and frequencies, Proc. 3rd ICBMFF Stuttgart, 1989, (61) 1-17.
10. J.F. Flavenot and N.Skalli, A critical depth criterion for the evaluation of long-life fatigue strength under multiaxial loading,Biaxial and Multiaxial Fatigue, EGF3, M.W.Brown and K. Miller, Ed., Mechanichal Engineering publications, London, 1989, 355-365.